った(P<0.4406, 繰り返しのある二元配置分散分析)。誤差は SEM である。

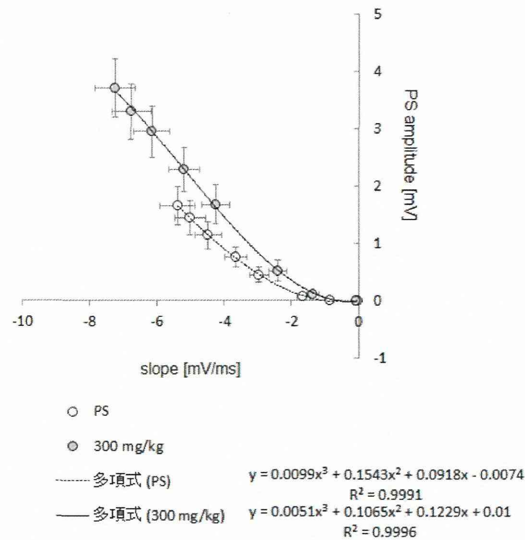

図 5. EPSP/Spike potentiation への VPA 曝露の影響
PND15 のときについて、CA1 錐体細胞の活動電位生成という出力応答を、樹状突起における入力応答の関数として解析した。8 段階の強さの電気刺激を与え、そのときの slope と PS 振幅の平均値と誤差をグラフ化した。図 1 に記載したように、slope と PS 振幅は曝露群で有意に増加している。近似曲線には、3 次の多項式を用い、近似式を記載した。1 次の傾きについて、対照群 0.0918、VPA 曝露群 0.1229 となり顕著な差は見られなかった。

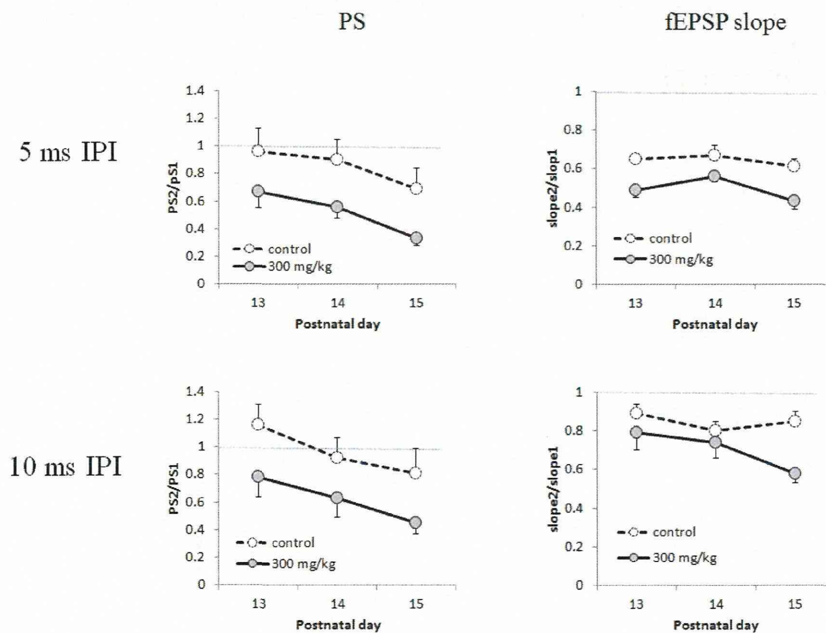

図 6. フィードバック抑制への VPA 曝露の影響
錐体細胞の細胞体層と樹状突起シナプス層へのフィードバック抑制について、PND13-15 で調べた。5, 10 ms いずれの刺激間隔においても、フィードバック抑制は増加しており、抑制性 GABA 機能が VPA 曝露によって亢進した。5 ms 刺激間隔のときの PS については p=0.0029, slope については p= 0.00004、 10 ms 刺激間隔のときの PS については、p= 0.0035, slope については p= 0.0018

となり、いずれも曝露の影響が顕著であった。曝露の影響の有無については、繰り返しのある二元配置分散分析で検定した。

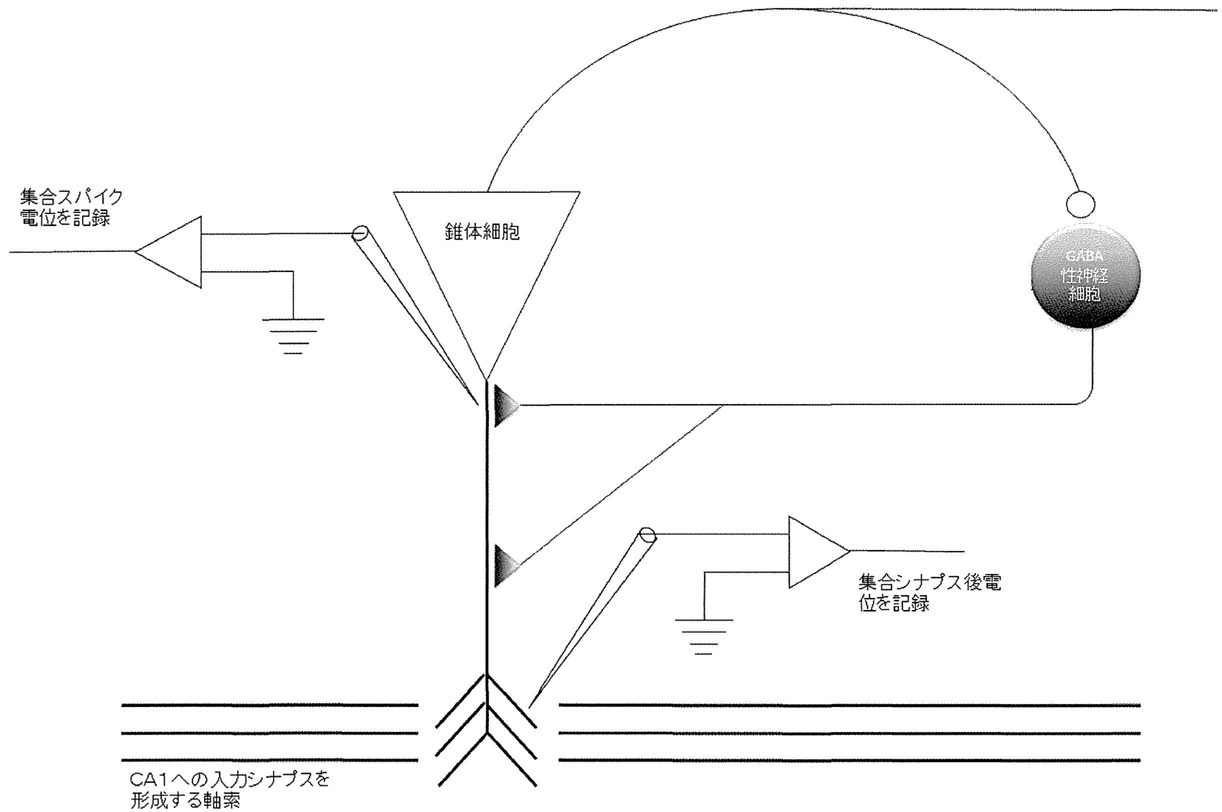

図 7. 海馬 CA1 領域におけるフィードバック抑制に寄与する GABA 性神経細胞と錐体細胞の神経連絡図と記録電極の位置
回路の説明については本文を参照のこと。

研究成果の刊行に関する一覧表

雑誌

発表者氏名	論文タイトル名	発表誌名	巻号	ページ	出版年
A. Oguchi-Katayama, A. Monma, Y. Sekino, Y, T. Moriguchi, K. Sato	Comparative gene expression analysis of the amygdalae of juvenile rats exposed to valproic acid at prenatal and postnatal stages.	J Toxicol Sci			印刷中
M. Kinoshita, K. Nasu-Tada, K. Fujishita, K. Sato, S. Koizumi	Secretion of matrix metalloproteinase-9 from astrocytes by inhibition of Tonic P2Y14-receptor-mediated signal(s).	Cell Mol Neurobiol	33:1	47-58	2013
J. Takaki, K. Fujimori, M. Miura, T. Suzuki, Y. Sekino, K. Sato	L-glutamate released from activated microglia downregulates astrocytic L-glutamate transporter expression in neuroinflammation: the 'collusion' hypothesis for increased extracellular L-glutamate concentration in neuroinflammation.	J Neuroinflammation	9	275	2012
Y. Morizawa, K. Sato, J. Takaki, A. Kawasaki, K. Shibata, T. Suzuki, S. Ohta, S. Koizumi	Cell-autonomous enhancement of glutamate-uptake by female astrocytes.	Mol Neurobiol	32:6	953-956	2012
F. Takata, S. Dohgu, A. Yamauchi, J. Matsumoto, T. Machida, K. Fujishita, K. Shibata, Y. Shinozaki, K. Sato, Y. Kataoka, S. Koizumi	In vitro blood-brain barrier models using brain capillary endothelial cells isolated from infant and adult rats retain age-related barrier properties.	PLoS ONE	8:1	e55166	2013
最上（重本） 由香里、佐藤 薫	ミクログリアの最近の話題～次々と明らかになるミクログリアの生理的新機能～	日薬理誌	140	216-220	2012
S. Yamada, Y. Kotake, Y. Sekino, Y. Kanda	AMP-activated protein kinase-mediated glucose transport as a novel target of tributyltin in human embryonic carcinoma cells.	Metallomics			印刷中
Y. Kanda	Cardiac differentiation of human iPS cells.	Nihon Yakurigaku Zasshi	141	32-36	2013
Y. Kanda	Cancer Stem Cells - Fact or Fiction? Role of Cancer Stem Cells in Cancer Biology and Therapy.	Science Publishers		1-22	2013

Y. Ihara, Y. Kanda, M. Seo, Y. Watanabe, T. Akamizu, Y. Tanaka	cAMP blocking but growth stimulating antibody; as another predisposing factor of Graves' disease (GD) -analysis using monoclonal TSH receptor antibodies derived from patients with GD.	Endocrine J	59	571-577	2012
T. Kuroda, S. Yasuda, S. Kusakawa, N. Hirata, Y. Kanda, K. Suzuki, M. Takahashi, S. Nishikawa, S. Kawamata, Y. Sato	Highly sensitive in vitro methods for detection of residual undifferentiated cells in retinal pigment epithelial cells derived from human induced pluripotent stem cells.	PLoS ONE	7	e37342	2012
W. Lin, N. Hirata, Y. Sekino, Y. Kanda	Role of α7-Nicotinic Acetylcholine Receptor in Normal and Cancer Stem Cells.	Current Drug Targets	13	656-665	2012
Y. Kanda	Cigarette smoke and breast cancer stem cells.	Journal of Women's Health Care	1	e104	2012
Y. Kanda	Isolation and characterization of cancer stem cells using flow cytometry.	Clinical Flow Cytometry – Emerging Applications		107-124	2012
諫田泰成	ヒト幹細胞を用いた医薬品の安全性評価	ファルマシア	48	862-867	2012
K. Kato, T. Shirao, H. Yamazaki K. Imamura, Y. Sekino	Regulation of AMPA receptor recruitment by the action binding protein drebrin in cultured hippocampal neurons.	J Neurosci Neuroengin eer	1	153-160	2012

研究成果の刊行物・別刷

Metallomics

RSC Publishing

PAPER

Cite this: DOI: 10.1039/c3mt20268b

AMP-activated protein kinase-mediated glucose transport as a novel target of tributyltin in human embryonic carcinoma cells†

Shigeru Yamada,[a] Yaichiro Kotake,[b] Yuko Sekino[a] and Yasunari Kanda*[a]

Received 28th December 2012,
Accepted 20th February 2013

DOI: 10.1039/c3mt20268b

www.rsc.org/metallomics

Organotin compounds such as tributyltin (TBT) are known to cause various forms of cytotoxicity, including developmental toxicity and neurotoxicity. However, the molecular target of the toxicity induced by nanomolar levels of TBT has not been identified. In the present study, we found that exposure to 100 nM TBT induced growth arrest in human pluripotent embryonic carcinoma cell line NT2/D1. Since glucose provides metabolic energy, we focused on the glycolytic system. We found that exposure to TBT reduced the levels of both glucose-6-phosphate and fructose-6-phosphate. To investigate the effect of TBT exposure on glycolysis, we examined glucose transporter (GLUT) activity. TBT exposure inhibited glucose uptake *via* a decrease in the level of cell surface-bound GLUT1. Furthermore, we examined the effect of AMP-activated protein kinase (AMPK), which is known to regulate glucose transport by facilitating GLUT translocation. Treatment with the potent AMPK activator, AICAR, restored the TBT-induced reduction in cell surface-bound GLUT1 and glucose uptake. In conclusion, these results suggest that exposure to nanomolar levels of TBT causes growth arrest by targeting glycolytic systems in human embryonic carcinoma cells. Thus, understanding the energy metabolism may provide new insights into the mechanisms of metal-induced cytotoxicity.

Introduction

Growing evidence suggests that environmental metals contribute to developmental toxicity and neurotoxicity.[1–3] Since the developing brain is inherently more vulnerable to injury than the adult brain, exposure to metals during early fetal development can potentially cause neurological disorders at doses much lower than those that are toxic in adults.[4–7] Therefore, it is necessary to elucidate the cytotoxic effects of such metals at low levels.

Organotin compounds are well known to cause cytotoxicity. Although organotin compounds or derivatives have been shown to have a potential anti-tumor activity[8,9] and some of them have already been entered into preclinical trials,[10] tributyltin (TBT) is considered to be associated with developmental toxicity and neurotoxicity.[11] For example, TBT can cause increased fetal mortality, decreased fetal birth weights, and behavioral abnormalities in rat offspring.[12,13] TBT is known to affect fertilization and embryonic development.[14] Moreover, TBT has been shown to induce neuronal death by glutamate excitotoxicity in cultured rat cortical neurons.[15] Although the use of TBT has already been restricted, butyltin compounds, including TBT, have been reported to be still present at concentrations between 50 and 400 nM in human blood.[16] However, the mechanism by which nanomolar levels of TBT cause cytotoxicity is not fully understood.

Glucose is the primary energy source for homeostasis. Glucose transport across the plasma membrane *via* a glucose transporter (GLUT) is a rate-limiting step in glucose metabolism.[17] AMP-activated protein kinase (AMPK), a serine threonine kinase, has been shown to regulate glucose uptake by facilitating the translocation of the GLUT to the membrane or by activation of transporter activity at the plasma membrane.[18,19] The fetal brain has been reported to rely on anaerobic glycolysis to meet its energy demands.[20] Thus, GLUT is considered essential in the early organogenesis period. GLUT1, a major subtype of GLUT in fetal tissue, has been shown to mediate organogenesis in rat embryos.[21] In addition, clinical data regarding human GLUT1 deficiency syndrome suggest that GLUT1 is necessary for human brain development.[22]

In the present study, we hypothesized a possible link between TBT toxicity and glucose metabolism. We found that

[a] *Division of Pharmacology, National Institute of Health Sciences, 1-18-1, Kamiyoga, Setagaya-ku 158-8501, Japan. E-mail: kanda@nihs.go.jp; Fax: +81-3-3700-9704; Tel: +81-3-3700-9704*

[b] *Department of Xenobiotic Metabolism and Molecular Toxicology, Graduate School of Biomedical and Health Sciences, Hiroshima University, Japan*

† Electronic supplementary information (ESI) available. See DOI: 10.1039/c3mt20268b

This journal is © The Royal Society of Chemistry 2013

exposure to TBT reduced the amounts of glucose-6-phosphate and fructose-6-phosphate *via* a decrease in surface-bound GLUT1 in the human pluripotent embryonic carcinoma cell line NT2/D1. In addition, treatment with the potent AMPK activator, 5-aminoimidazole-4-carboxyamide ribonucleoside (AICAR), restored the inhibitory effect of TBT on both cell surface-bound GLUT1 levels and glucose uptake. We report here that the glycolytic pathway is a molecular target of nanomolar levels of TBT in human embryonic carcinoma cells.

Methods

Cell culture

NT2/D1 cells were obtained from the American Type Culture Collection. The cells were cultured in Dulbecco's modified Eagle's medium (DMEM; Sigma-Aldrich, St. Louis, MO, USA) supplemented with 10% fetal bovine serum (FBS; Biological Industries, Ashrat, Israel) and 0.05 mg mL^{-1} penicillin–streptomycin mixture (Life Technologies, Carlsbad, CA, USA) at 37 °C and 5% CO_2. For neural differentiation, all-trans retinoic acid (RA; Sigma-Aldrich) was added to the medium twice a week at a final concentration of 10 μM.

Cell proliferation assay

Cell viability was measured using the CellTiter 96 AQueous One Solution Cell Proliferation Assay (Promega, Madison, WI, USA), according to the manufacturer's instructions. Briefly, NT2/D1 cells were seeded into 96-well plates and exposed to different concentrations of TBT. After exposure to TBT, One Solution Reagent was added to each well, and the plate was incubated at 37 °C for another 2 h. Absorbance was measured at 490 nm using an iMark microplate reader (Bio-Rad, Hercules, CA, USA).

Glucose uptake assay

A glucose uptake assay was performed using a fluorescent glucose derivative, 2-[*N*-(7-nitrobenz-2-oxa-1,3-diazol-4-yl)amino]-2-deoxy-D-glucose (2-NBDG; Peptide Institute Inc., Osaka, Japan) by the previously reported procedure with slight modifications.[23] Briefly, NT2/D1 cells exposed to TBT were incubated with 2-NBDG (100 μM) for 2 h at 37 °C. The 2-NBDG uptake reaction was stopped by draining the incubation medium and washing the cells twice with ice-cold PBS. The incorporated 2-NBDG was measured using a Wallac1420ARVO fluoroscan (Perkin-Elmer, Waltham, MA, USA) with excitation at 488 nm and emission at 515 nm. The fluorescence intensities were normalized to the total protein content.

Hexokinase activity assay

Hexokinase activity was determined using a commercial Hexokinase Colorimetric Assay Kit (Biovision, Mountain View, CA, USA), according to the manufacturer's instructions.

AMPK activity assay

AMPK activity was determined using a commercial CycLex AMP Kinase Assay Kit (MBL International, Woburn, MA, USA), according to the manufacturer's instructions.

Determination of glucose-6-phosphate and fructose-6-phosphate

Intracellular metabolites were extracted and used for subsequent capillary electrophoresis time-of-flight mass spectrometry (CE-TOFMS) analysis, as described previously.[24] Glucose-6-phosphate and fructose-6-phosphate were determined using an Agilent CE capillary electrophoresis system (Agilent Technologies, Waldbronn, Germany) equipped with an Agilent G3250AA LC/MSD TOF system (Agilent Technologies, Palo Alto, CA), an Agilent 1100 series isocratic HPLC pump, a G1603A Agilent CE-MS adapter kit, and a G1607A Agilent CE-electrospray ionization 53-MS sprayer kit. For system control and data acquisition, G2201AA Agilent ChemStation software was used for CE, and Agilent TOF (Analyst QS) software was used for TOFMS.

Western blotting

Western blotting was performed as previously reported.[25] Briefly, the cells were lysed using Cell Lysis Buffer (Cell Signaling Technology, Danvers, MA, USA), and proteins were then separated by sodium dodecyl sulfate (SDS)-polyacrylamide gel electrophoresis and electrophoretically transferred to Immobilon-P membranes (Millipore, Billerica, MA, USA). The membranes were probed using primary antibodies (anti-GLUT1 polyclonal antibodies [1:200; Santa Cruz Biotechnology, Santa Cruz, CA, USA], anti-c-Myc polyclonal antibodies [1:1000; Sigma-Aldrich], anti-Flag monoclonal antibodies [1:1000; Sigma-Aldrich], and anti-β-actin monoclonal antibodies [1:1000; Sigma-Aldrich]). The membranes were then incubated with secondary antibodies against rabbit or mouse IgG conjugated with horseradish peroxidase (Cell Signaling Technology). The bands were visualized using an ECL Western Blotting Analysis System (GE Healthcare, Buckinghamshire, UK), and images were acquired using a LAS-3000 Imager (Fujifilm UK Ltd., Systems, Bedford, UK). The density of each band was quantified with ImageJ software (NIH, Bethesda, MD, USA).

Cell surface biotinylation

NT2/D1 cell surface proteins were biotinylated using a Cell Surface Protein Isolation Kit, according to the manufacturer's instructions (Pierce, Rockford, IL, USA). Briefly, cells were incubated with ice-cold phosphate-buffered saline (PBS; pH 7.4) containing Sulfo-NHS-SS-Biotin, with gentle rocking for 30 min at 4 °C. The biotinylated proteins were precipitated with streptavidin beads and eluted from the beads with SDS sample buffer. The proteins were analyzed by western blotting with anti-GLUT1 antibodies.

Immunohistochemistry

Cells, cultured on glass coverslips, were fixed in 4% paraformaldehyde in PBS (pH 7.4) for 15 min at room temperature. The fixed cells were incubated with anti-GLUT1 polyclonal antibodies (1:100; Santa Cruz) for 1 h at room temperature. Finally, they were incubated with Alexa488-conjugated secondary antibodies (1:200; Life Technologies) for 1 h at room temperature. The cells were enclosed in SlowFade (Life Technologies) and examined under a BIOREVO BZ-9000 fluorescent microscope (Keyence, Osaka, Japan).

This journal is © The Royal Society of Chemistry 2013

Transfection

Cells were transiently transfected with Flag-tagged GLUT1 in pEF6 (a kind gift from Dr Rathmell) and c-Myc-tagged constitutively active-AMPK-α1 (T172D) or c-Myc-tagged dominant-negative-AMPK-α1 (K45R) in pcDNA3 (a kind gift from Dr Carling) using the FuGene HD Transfection Reagent (Promega), according to the manufacturer's protocol. After 48 h incubation, the transfectants were cultured with 12.5 μg mL^{-1} blasticidin or 0.5 mg mL^{-1} G418.

Real-time PCR

After total RNA was isolated from NT2/D1 cells using TRIzol (Life Technologies), quantitative real-time reverse transcription (RT)-PCR with a QuantiTect SYBR Green RT-PCR Kit (QIAGEN, Valencia, CA, USA) was performed using an ABI PRISM 7900HT sequence detection system (Applied Biosystems, Foster City, CA, USA), as previously reported.[26] The relative changes in the amounts of transcripts in each sample were normalized using ribosomal protein L13 (RPL13) mRNA levels. The sequences of the primers used for real-time PCR analysis are as follows: GLUT1 (forward, 5′-CCAGCTGCCATTGCCGTT-3′; reverse, 5′-GACGTAGGGACCACACAGTTGC-3′), GLUT2 (forward, 5′-CACACAAGACCTGGAATTGACA-3′; reverse, 5′-CGGTCATCCAGTGGAACAC-3′), GLUT3 (forward, 5′-CAATGCTCCTGAGAAGATCATAA-3′; reverse, 5′-AAAGCGGTTGACGAAGAGT-3′), GLUT4 (forward, 5′-CTGGGCCTCACAGTGCTAC-3′; reverse, 5′-GTCAGGCGCTTCAGACTCTT-3′), nestin (forward, 5′-GGCAGCGTTGGAACAGAGGT-3′; reverse, 5′-CATCTTGAGGTGCGCCAGCT-3′), NeuroD (forward, 5′-GGAAACGAACCCACTGTGCT-3′; reverse, 5′-GCCACACCAAATTCGTGGTG-3′), Math1 (forward, 5′-GTCCGAGCTGCTACAAACG-3′; reverse, 5′-GTGGTGGTGGTCGCTTTT-3′), MAP2 (forward, 5′-CCAATGGATTCCCATACAGG-3′; reverse, 5′-CTGCTACAGCCTCAGCAGTG-3′), RPL13 (forward, 5′-CATCGTGGCTAAACAGGTACTG-3′; reverse, 5′-GCACGACCTTGAGGGCAGCC-3′).

Materials

TBT was obtained from Tokyo Chemical Industry (Tokyo, Japan). Tin acetate (TA), AICAR, and rosiglitazone were obtained from Sigma-Aldrich. All other reagents were of analytical grade and obtained from commercial sources.

Statistical analysis

All data were presented as mean ± S.D. ANOVA followed by a *post hoc* Tukey test was used to analyze data in Fig. 1–4. Unpaired Student's *t* test was used to analyze data in Fig. 5. A *p* value of less than 0.05 was considered significant.

Results

To examine the effect of TBT on the proliferation of human NT2/D1 embryonic carcinoma cells, we exposed the cells to different concentrations of TBT for 24 h and measured cell viability by MTT assay. Treatment with TBT reduced cell viability in a dose-dependent manner (Fig. 1A; 0.03–0.3 μM). We observed that almost all cells were detached from the culture dish at TBT concentrations of 300 nM and above. In contrast, the less toxic TA had little effect at any concentration (Fig. 1A–e). We performed time-course experiments with 100 nM TBT, and determined the cell number. Exposure to

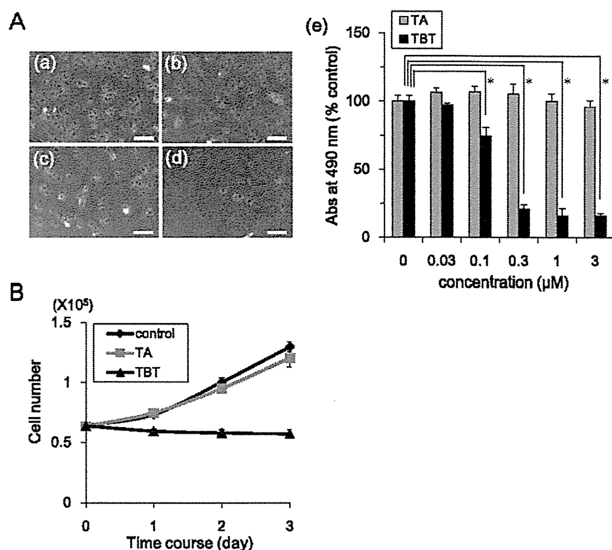

Fig. 1 Effect of TBT exposure on cell proliferation in NT2/D1 cells. (A) NT2/D1 cells were seeded into 96-well plates and exposed to TBT at different concentrations for 24 h. (a–d) Phase-contrast photomicrographs of NT2/D1 cells exposed to TBT at 0, 0.03, 0.1, or 0.3 μM (Bar = 100 μm). (e) Cell viability in the presence of TBT or TA was examined using the CellTiter 96 AQueous One Solution Cell Proliferation Assay. (B) NT2/D1 cells (6 × 10^5 cells) were seeded into 100 mm dishes and exposed to 100 nM TBT. After 24, 48, and 72 h, cell count was determined using a hemocytometer. *$P < 0.05$.

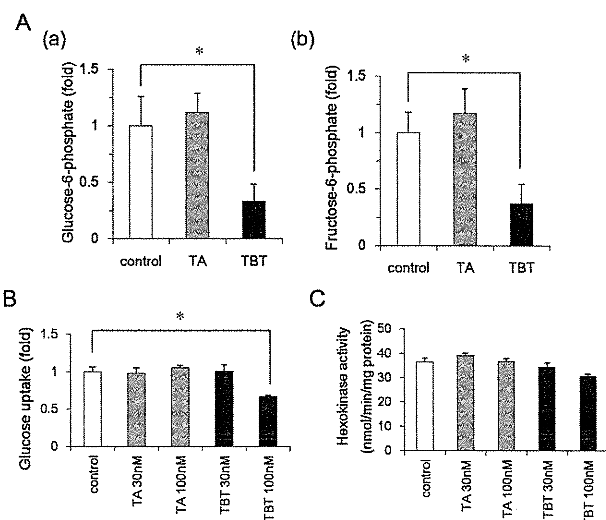

Fig. 2 Effect of TBT exposure on glycolytic systems in NT2/D1 cells. (A) After 24 h exposure to 100 nM TBT or TA, glucose 6-phosphate (a) and fructose 6-phosphate (b) levels were determined using CE-TOFMS. (B) After exposure to TBT or TA (30, 100 nM) for 24 h, glucose uptake assay was performed using a fluorescent glucose analog 2-NBDG. The fluorescence intensities of incorporated 2-NBDG were normalized to total cellular protein content. (C) After exposure to TBT or TA (30, 100 nM) for 24 h, hexokinase activity was measured using a commercial assay kit. *$P < 0.05$.

This journal is © The Royal Society of Chemistry 2013

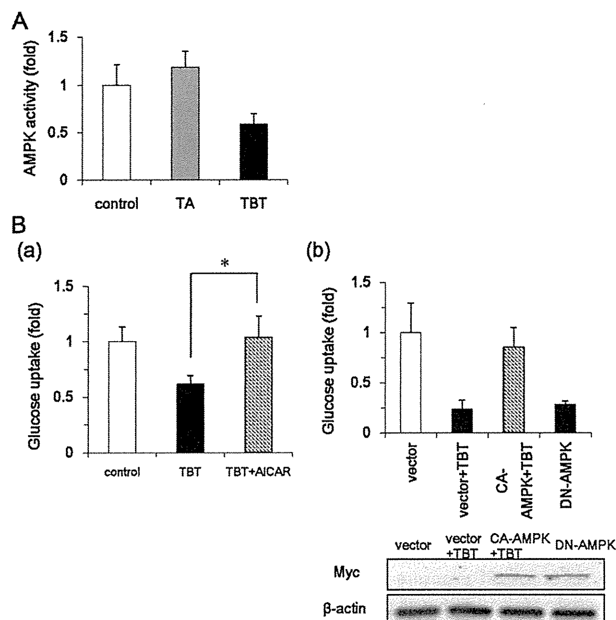

Fig. 3 Effect of AMPK on glucose uptake in NT2/D1 cells. (A) NT2/D1 cells were exposed to TBT or TA at 100 nM for 24 h. AICAR (0.5 mM) treatment was performed for 3 h. AMPK activity in the lysed cells was determined using a commercial assay kit. (B) NT2/D1 cells were exposed to TBT in the presence of 0.5 mM AICAR. (C) After overexpression of constitutively active (CA) mutants of AMPK, NT2/D1 cells were exposed to 100 nM TBT for 24 h, and glucose uptake assay was performed. After overexpression of dominant-negative (DN) mutants of AMPK, basal glucose uptake was tested. A glucose uptake assay was performed using the fluorescent glucose analog 2-NBDG. The fluorescence intensities of incorporated 2-NBDG were normalized to total cellular protein content. $^*P < 0.05$.

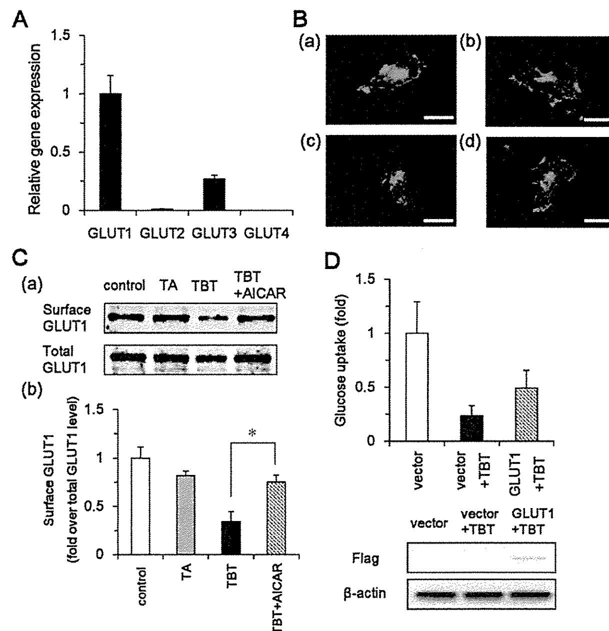

Fig. 4 Effect of TBT exposure on GLUT1 localization in NT2/D1 cells. (A) Expression of GLUT family by real-time PCR in NT2/D1 cells. Relative changes were determined by normalizing to RPL13. (B) After exposure to 100 nM TBT for 24 h, NT2/D1 cells were immunostained with anti-GLUT1 polyclonal antibodies. (a) Control, (b) 100 nM TA, (c) 100 nM TBT, and (d) 100 nM TBT + 0.5 mM AICAR. (Bar = 25 μm). (C) (a) NT2/D1 cell surface proteins were biotinylated using Sulfo-NHS-SS-Biotin, and then lysed. After precipitation with streptavidin beads, biotinylated proteins were analyzed by western blotting using anti-GLUT1 antibodies. Total GLUT1 protein was detected in cell lysate. (b) The relative density of bands was quantified with ImageJ software. Cell surface GLUT1 levels were normalized to total GLUT1 levels. (D) After overexpression of GLUT1, NT2/D1 cells were exposed to 100 nM TBT for 24 h, and glucose uptake assay was performed using the fluorescent glucose analog 2-NBDG. The fluorescence intensities of incorporated 2-NBDG were normalized to total cellular protein content. $^*P < 0.05$.

TBT suppressed the growth curve, but the total cell number did not alter throughout the time-course experiment (Fig. 1B). These data suggest that exposure to 100 nM TBT induced growth arrest in the cells without causing cell death.

Glucose provides metabolic energy for cell growth and it is incorporated by glucose transporters.[17] To examine the mechanism by which TBT induces growth arrest at low concentrations, we determined the glucose-6-phosphate, a major metabolite in glycolysis. We found that exposure to 100 nM TBT reduced the amount of glucose-6-phosphate (Fig. 2A). Fructose-6-phosphate, which is produced by isomerization of glucose 6-phosphate, also reduced by TBT. To check whether the decrease in glucose-6-phosphate is induced by inhibition of glucose transport, we examined the activity of glucose uptake by using 2-NBDG, a fluorescently labeled 2-deoxyglucose. Similar to the cell growth, glucose uptake was significantly inhibited by 100 nM TBT, not by 30 nM TBT (Fig. 2B). TA had little effect on glucose uptake. To examine whether the inhibition is regulated by transcription, we tested the effect of short-term exposure. Exposure to TBT for 1 h suppressed glucose uptake (Fig. S1, ESI†), suggesting that gene expression is not involved in the effect of TBT. Since TBT has been shown to activate transcriptional activity of peroxisome proliferator-activated receptor γ (PPARγ),[27,28] we tested the effect of the PPARγ agonist rosiglitazone on the glucose uptake. Treatment with rosiglitazone increased glucose uptake (Fig. S2, ESI†), suggesting that PPARγ is not involved in TBT-induced inhibition of glucose uptake. Furthermore, we examined the activity of hexokinase, which catalyzes the phosphorylation of glucose into glucose-6-phosphate. As shown in Fig. 2C, hexokinase activity was not significantly altered by TBT. Exposure to TA also produced similar results. These data suggest that TBT exposure decreases the amount of glycolytic metabolites *via* inhibition of glucose transport.

AMP-activated protein kinase (AMPK) is known to regulate the translocation of a glucose transporter (GLUT) to the plasma membrane.[29] We examined whether AMPK is involved in the inhibition of glycolytic systems by TBT exposure. Exposure to 100 nM TBT reduced AMPK activity (Fig. 3A). In contrast, TA had little effect on AMPK. In addition, treatment with AICAR (a potent AMPK activator) recovered the inhibitory effect of TBT on glucose uptake (Fig. 3B). To confirm the effect of AICAR, we examined the effect of constitutively active (CA) mutants of AMPK. Similar to the treatment with AICAR, overexpression of CA-AMPK recovered the inhibitory effect of TBT on glucose uptake. Overexpression of dominant-negative mutants of AMPK reduced the basal level of glucose uptake, suggesting that

 This journal is © The Royal Society of Chemistry 2013

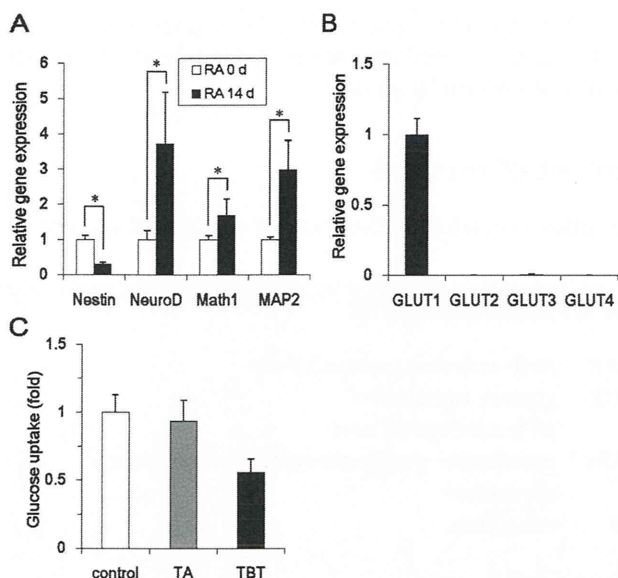

Fig. 5 Effect of neuronal induction on glucose uptake under TBT exposure in NT2/D1 cells. (A) To induce neuronal differentiation, NT2/D1 cells were treated with 10 μM RA for 14 days. The relative expression of neuronal markers (NeuroD, Math1, and MAP2) and a marker of undifferentiation (nestin) were measured by real-time-PCR. The relative changes were normalized to RPL13. (B) Expressions of members of the GLUT family were measured by real-time PCR in differentiated NT2/D1 cells. Relative changes were determined by normalizing to RPL13. (C) After exposure to 100 nM TBT for 24 h, glucose uptake was measured in differentiated cells. The fluorescence intensities of intracellularly incorporated 2-NBDG were measured and normalized to the total cellular protein levels. $^{*}P < 0.05$.

glucose uptake is AMPK-dependent in NT2/D1 cells. Taken together, these data suggest that TBT exposure suppresses glucose uptake through the inhibition of AMPK activity.

We next examined the mechanism by which AMPK regulates glucose uptake in NT2/D1 cells. Real-time PCR analysis showed that GLUT1 was a major subtype in NT2/D1 cells (Fig. 4A). Since TBT exposure did not affect gene expression of GLUT1 (data not shown), we examined GLUT1 localization by immunohistochemistry. Expression of GLUT1 was observed at the plasma membrane and in the intracellular segment (Fig. 4B). Exposure with TBT reduced the cell surface expression of GLUT1. Treatment with AICAR recovered the inhibitory effect of TBT. To confirm these observations using microscopy, we labeled cell surface-bound GLUT1 by biotinylation of cell surface proteins (Fig. 4C). Using this approach, we determined that TBT exposure reduced the amount of cell surface-bound GLUT1. AICAR reversed this inhibitory effect of TBT. Furthermore, overexpression of GLUT1 partially recovered the TBT-induced inhibition of glucose uptake (Fig. 4D). These data suggest that TBT inhibits glucose uptake mediated by cell surface translocation of GLUT1, a process dependent on AMPK.

To examine whether the effect of TBT was selective for embryonic cells, we used NT2/D1 cells differentiated by retinoic acid.[30] Real-time PCR analysis revealed that RA-treated NT2/D1 cells showed upregulated expression of markers of differentiation (NeuroD, Math1, MAP2) and downregulated expression of a marker of undifferentiation (nestin), confirming the induction of differentiation (Fig. 5A). Real-time PCR confirmed that GLUT1 is a major subtype in the differentiated NT2/D1 cells (Fig. 5B). Furthermore, exposure to 100 nM TBT also reduced glucose uptake in differentiated NT2/D1 cells. In contrast, TA had little effect (Fig. 5C). These data suggest that TBT suppresses glucose uptake in both undifferentiated and differentiated cells.

Discussion

In the present study, we showed that the glycolytic pathway is a novel target of TBT toxicity in human embryonic carcinoma cells. We showed that TBT suppresses AMPK-dependent glucose uptake, and thereby, the amount of glucose-6-phosphate. The inhibitory effects of TBT on glycolytic systems would lead to growth arrest in the cells. Fig. 6 shows a proposed model of TBT-induced toxicity, based on the data observed in our study.

Our studies showed that treatment with 1 μM TBT resulted in the death of human embryonic carcinoma cells (Fig. 1). Consistent with these observations, previous studies have shown that micromolar levels of TBT induce apoptosis in various cells such as human amnion cells,[31] hepatocytes,[32] and neutrophils.[33] In contrast, exposure to 100 nM TBT resulted in neither growth arrest nor cell death. Therefore, we focused on intracellular metabolites as potential mediators of TBT-induced growth arrest. We found that exposure to nanomolar levels of TBT affects the intracellular metabolic balance and decreases the amount of glucose metabolites (Fig. 2). A previous report showed that the organotin compounds such as TBT might be present in human blood at nanomolar levels.[16] Glucose metabolism analysis revealed novel toxic mechanisms

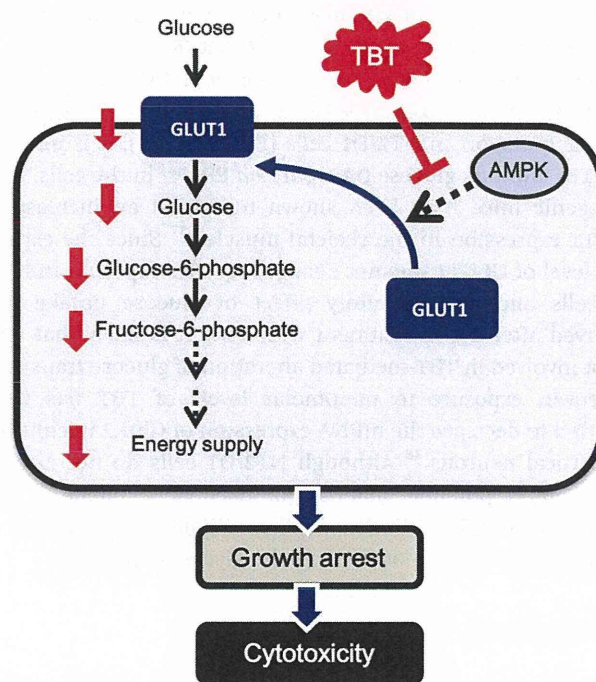

Fig. 6 Proposed model of TBT toxicity in human embryonic carcinoma cells.

for the toxicity of nanomolar levels of TBT. Thus, the glycolytic pathway might account for the unknown toxic mechanism induced by heavy metal exposure.

Our data suggest that the target molecule of TBT toxicity is GLUT1, a major subtype of GLUT in NT2/D1 cells (Fig. 4). Since the expression of GLUT1 is observed in a broad range of cell types, the toxicity of TBT may also be observed in other cells. For example, we showed that TBT reduces glucose uptake in differentiated NT2/D1 cells, which express GLUT1 (Fig. 5). Thus, it is possible that TBT induces toxicity in mature neurons *via* inhibition of GLUT function.

We showed that TBT decreases AMPK activity, one of the GLUT regulators, in NT2/D1 cells (Fig. 3). In addition, overexpression of AMPK or the AMPK activator restored the glucose uptake, confirming that AMPK is a possible target of TBT. In contrast, 500 nM TBT has been shown to increase AMPK phosphorylation in rat cortical neurons.[34] This discrepancy might be due to the concentration of TBT or different types of cells.

Several studies suggest that TBT directly interacts with target enzymes. TBT at a concentration of 10–100 nM has been shown to act as an agonist of PPARγ and the retinoid X receptor (RXR) because of its higher binding affinity compared to intrinsic ligands. Other studies reported that micromolar concentrations of TBT inhibit F1F0 ATP synthase and 11β-hydroxysteroid dehydrogenase by direct interaction.[35,36] Therefore, TBT can bind to multiple targets with broad specificity. It is possible that TBT also interacts with AMPK. On the other hand, calmodulin-dependent protein kinase II (CaMK II) and serine–threonine liver kinase B1 (LKB1) have been shown to phosphorylate AMPK and cause subsequent activation of glucose transport.[29] Furthermore, there may be an additional signaling molecule between TBT and AMPK. It remains to be elucidated how TBT regulates AMPK in embryonic carcinoma cells.

Nanomolar levels of TBT may interact with several targets in other types of cells, such as PPARγ, RXR, and α-amino-3-hydroxy-5-methylisoxazole-4-propionic acid (AMPA) receptors 2 (GluR2). Since rosiglitazone, a PPARγ agonist, increased glucose transport in NT2/D1 cells (Fig. S2, ESI†), it is unlikely that TBT inhibits glucose transport *via* PPARγ in the cells. RXR transgenic mice have been shown to exhibit an increase in GLUT1 expression in the skeletal muscles.[37] Since the expression level of GLUT1 was not changed by TBT exposure in NT2/D1 cells and the inhibitory effect of glucose uptake was observed after a 1 h treatment with TBT, it is likely that RXR is not involved in TBT-mediated alteration of glucose transport. Moreover, exposure to nanomolar levels of TBT has been reported to decrease the mRNA expression of GluR2 in cultured rat cortical neurons.[38] Although NT2/D1 cells do not express GluR2, it is possible that GluR2 may be a target in the differentiated NT2/D1 cells. Further studies are required to examine these targets other than the glycolytic pathway.

Conclusions

We found that exposure to nanomolar levels of TBT mainly targets the glycolytic systems in human embryonic carcinoma cells. Thus, glycolytic systems may be a good target for previously unknown mechanisms of toxicity induced by metal exposure at nanomolar levels.

Conflict of interest

The authors declare that there are no conflicts of interest.

List of abbreviations

AMPK	AMP-activated protein kinase
GLUT	glucose transporter
RA	all-trans retinoic acid
PPARγ	peroxisome proliferator-activated receptor γ
TA	tin acetate
TBT	tributyltin

Acknowledgements

We would like to thank Dr Rathmell and Dr Carling for providing the materials. This study was supported in part by a Health and Labour Sciences Research Grant from the Ministry of Health, Labour and Welfare, Japan (Y. Ka.), a grant from the Program for Promotion of Fundamental Studies in Health Sciences of the National Institute of Biomedical Innovation (NIBIO) (No. 09-02 to Y. Ka.), Grants-in-Aid for Scientific Research (No. 23590322 to Y. Ka. and No. 23310047 to Y. Ko.) from the Japan Society for the Promotion of Science, and a grant from the Smoking Research Foundation (Y. Ka.).

References

1 H. L. Needleman, C. Gunnoe, A. Leviton, R. Reed, H. Peresie, C. Maher and P. Barrett, Deficits in psychologic and classroom performance of children with elevated dentine lead levels, *N. Engl. J. Med.*, 1979, **300**, 689–695.

2 G. Winneke, Developmental aspects of environmental neurotoxicology: lessons from lead and polychlorinated biphenyls, *J. Neurol. Sci.*, 2011, **308**, 9–15.

3 L. G. Costa, M. Aschne, A. Vitalone, T. Syversen and O. P. Soldin, Developmental neuropathology of environmental agents, *Annu. Rev. Pharmacol. Toxicol.*, 2004, **44**, 87–110.

4 J. Dobbing, *Vulnerable periods in developing brain*, in *Appl. Neurochem.*, ed. A. N. Davison and J. Dobbing, Davis, Philadelphia, 1968, pp. 287–316.

5 P. M. Rodier, Developing brain as a target of toxicity, *Environ. Health Perspect.*, 1995, **103**(suppl 6), 73–76.

6 D. Rice and S. Barone Jr, Critical periods of vulnerability for the developing nervous system: evidence from humans and animal models, *Environ. Health Perspect.*, 2000, **108**(suppl 3), 511–533.

7 H. Asakawa, M. Tsunoda, T. Kaido, M. Hosokawa, C. Sugaya, Y. Inoue, Y. Kudo, T. Satoh, H. Katagiri, H. Akita, M. Saji, M. Wakasa, T. Negishi, T. Tashiro and Y. Aizawa, Enhanced

 This journal is © The Royal Society of Chemistry 2013

inhibitory effects of TBT chloride on the development of F1 rats, *Arch. Environ. Contam. Toxicol.*, 2010, **58**, 1065–1073.

8 S. Gómez-Ruiz, G. N. Kaluderović, S. Prashar, E. Hey-Hawkins, A. Erić, Z. Zizak and Z. D. Juranić, Study of the cytotoxic activity of di and triphenyltin(IV) carboxylate complexes, *J. Inorg. Biochem.*, 2008, **102**, 2087–2096.

9 L. Rocamora-Reverte, E. Carrasco-García, J. Ceballos-Torres, S. Prashar, G. N. Kaluđerović, J. A. Ferragut and S. Gómez-Ruiz, Study of the anticancer properties of tin(IV) carboxylate complexes on a panel of human tumor cell lines, *ChemMedChem*, 2012, 7, 301–310.

10 A. González, E. Gómez, A. Cortés-Lozada, S. Hernández, T. Ramírez-Apan and A. Nieto-Camacho, Heptacoordinate tin(IV) compounds derived from pyridine Schiff bases: synthesis, characterization, *in vitro* cytotoxicity, anti-inflammatory and antioxidant activity, *Chem. Pharm. Bull.*, 2009, **57**, 5–15.

11 Y. Kotake, Molecular mechanisms of environmental organotin toxicity in mammals, *Biol. Pharm. Bull.*, 2012, **35**, 1876–1880.

12 T. Noda, S. Morita, T. Yamano, M. Shimizu, T. Nakamura, M. Saitoh and A. Yamada, Teratogenicity study of tri-*n*-butyltin acetate in rats by oral administration, *Toxicol. Lett.*, 1991, **55**, 109–115.

13 A. T. Gardlund, T. Archer, K. Danielsen, B. Danielsson, A. Frederiksson, N. G. Lindquist, H. Lindstrom and J. Luthman, Effects of prenatal exposure to tributyltin and trihexyltin on behavior in rats, *Neurotoxicol. Teratol.*, 1991, **13**, 99–105.

14 Q. Li, M. Osada, K. Takahashi, T. Matsutani and K. Mori, Accumulation and depuration of tributyltin oxide and its effect on the fertilization and embryonic development in the pacific oyster, *Crassostrea gigas*, *Bull. Environ. Contam. Toxicol.*, 1997, **58**, 489–496.

15 Y. Nakatsu, Y. Kotake, K. Komasaka, H. Hakozaki, R. Taguchi, T. Kume, A. Akaike and S. Ohta, Glutamate excitotoxicity is involved in cell death caused by tributyltin in cultured rat cortical neurons, *Toxicol. Sci.*, 2006, **89**, 235–242.

16 M. M. Whalen, B. G. Loganathan and K. Kannan, Immunotoxicity of environmentally relevant concentrations of butyltins on human natural killer cells *in vitro*, *Environ. Res. Lett.*, 1999, **81**, 108–116.

17 L. Pellerin, Food for thought: the importance of glucose and other energy substrates for sustaining brain function under varying levels of activity, *Diabetes Metab.*, 2010, **36**, S59–S63.

18 K. Barnes, J. C. Ingram, O. H. Porras, L. F. Barros, E. R. Hudson, L. G. Fryer, F. Foufelle, D. Carling, D. G. Hardie and S. A. Baldwin, Activation of GLUT1 by metabolic and osmotic stress: potential involvement of AMP-activated protein kinase (AMPK), *J. Cell Sci.*, 2002, **115**, 2433–2442.

19 M. Jing, V. K. Cheruvu and F. Ismail-Beigi, Stimulation of glucose transport in response to activation of distinct AMPK signaling pathways, *Am. J. Physiol.: Cell Physiol.*, 2008, **295**, C1071–C1082.

20 B. Kunievsky, J. Pretsky and E. Yavin, Transient rise of glucose uptake in the fetal rat brain after brief episodes of intrauterine ischemia, *Dev. Neurosci.*, 1994, **16**, 313–320.

21 K. Matsumoto, S. Akazawa, M. Ishibashi, R. A. Trocino, H. Matsuo, H. Yamasaki, Y. Yamaguchi, S. Nagamatsu and S. Nagataki, Abundant expression of GLUT1 and GLUT3 in rat embryo during the early organogenesis period, *Biochem. Biophys. Res. Commun.*, 1995, **209**, 95–102.

22 P. J. Jensen, J. D. Gitlin and M. O. Carayannopoulos, GLUT1 deficiency links nutrient availability and apoptosis during embryonic development, *J. Biol. Chem.*, 2006, **281**, 13382–13387.

23 Y. Kanda and Y. Watanabe, Thrombin-induced glucose transport *via* Src-p38 MAPK pathway in vascular smooth muscle cells, *Br. J. Pharmacol.*, 2005, **146**, 60–67.

24 T. Soga, Y. Ueno, H. Naraoka, Y. Ohashi, M. Tomita and T. Nishioka, Simultaneous determination of anionic intermediates for *Bacillus subtilis* metabolic pathways by capillary electrophoresis electrospray ionization mass spectrometry, *Anal. Chem.*, 2002, **74**, 2233–2239.

25 Y. Kanda and Y. Watanabe, Adrenaline increases glucose transport *via* a Rap1-p38MAPK pathway in rat vascular smooth muscle cells, *Br. J. Pharmacol.*, 2007, **151**, 476–482.

26 N. Hiarta, Y. Sekinoa and Y. Kanda, Nicotine increases cancer stem cell population in MCF-7 cells, *Biochem. Biophys. Res. Commun.*, 2010, **403**, 138–143.

27 T. Kanayama, N. Kobayashi, S. Mamiya, T. Nakanishi and J. Nishikawa, Organotin compounds promote adipocyte differentiation as agonists of the peroxisome proliferator-activated receptor gamma/retinoid X receptor pathway, *Mol. Pharmacol.*, 2005, **67**, 766–774.

28 F. Grün, H. Watanabe, Z. Zamanian, L. Maeda, K. Arima, R. Cubacha, D. M. Gardiner, J. Kanno, T. Iguchi and B. Blumberg, Endocrine-disrupting organotin compounds are potent inducers of adipogenesis in vertebrates, *Mol. Endocrinol.*, 2006, **20**, 2141–2155.

29 D. G. Hardie, F. A. Ross and S. A. Hawley, AMPK: a nutrient and energy sensor that maintains energy homeostasis, *Nat. Rev. Mol. Cell Biol.*, 2012, **13**, 251–262.

30 S. J. Pleasure, C. Page and V. M. Lee, Pure, postmitotic, polarized human neurons derived from NTera 2 cells provide a system for expressing exogenous proteins in terminally differentiated neurons, *J. Neurosci.*, 1992, **12**, 1802–1815.

31 X. Zhu, M. Xing, J. Lou, X. Wang, W. Fu and L. Xu, Apoptotic related biochemical changes in human amnion cells induced by tributyltin, *Toxicology*, 2007, **230**, 45–52.

32 M. Grondin, M. Marion, F. Denizeau and D. A. Averill-Bate, Tributyltin induces apoptotic signaling in hepatocytes through pathways involving the endoplasmic reticulum and mitochondria, *Toxicol. Appl. Pharmacol.*, 2007, **222**, 57–68.

33 V. Lavastre and D. Girard, Tributyltin induces human neutrophil apoptosis and selective degradation of cytoskeletal proteins by caspases, *J. Toxicol. Environ. Health, Part A*, 2002, **65**, 1013–1024.

34 Y. Nakatsu, Y. Kotake, A. Hino and S. Ohta, Activation of AMP-activated protein kinase by tributyltin induces neuronal cell death, *Toxicol. Appl. Pharmacol.*, 2008, **230**, 358–363.
35 C. von Ballmoos, J. Brunner and P. Dimroth, The ion channel of F-ATP synthase is the target of toxic organotin compounds, *Proc. Natl. Acad. Sci. U. S. A.*, 2004, **101**, 11239–11244.
36 A. G. Atanasov, L. G. Nashev, S. Tam, M. E. Baker and A. Odermatt, Organotins disrupt the 11β-hydroxysteroid dehydrogenase type 2-dependent local inactivation of glucocorticoids, *Environ. Health Perspect.*, 2005, **113**, 1600–1606.
37 S. Sugita, Y. Kamei, F. Akaike, T. Suganami, S. Kanai, M. Hattori, Y. Manabe, N. Fujii, T. Takai-Igarashi, M. Tadaishi, J. Oka, H. Aburatani, T. Yamada, H. Katagiri, S. Kakehi, Y. Tamura, H. Kubo, K. N. S. Miura, O. Ezaki and Y. Ogawa, Increased systemic glucose tolerance with increased muscle glucose uptake in transgenic mice overexpressing RXRγ in skeletal muscle, *PLoS One*, **6**, e20467.
38 Y. Nakatsu, Y. Kotake Y, T. Takishit and S. Ohta, Long-term exposure to endogenous levels of tributyltin decreases GluR2 expression and increases neuronal vulnerability to glutamate, *Toxicol. Appl. Pharmacol.*, 2009, **240**, 292–298.

 This journal is © The Royal Society of Chemistry 2013